molbank

MDPI

Communication

Coordination of *O*-Propyl-*N*-phenylthiocarbamate to HgI_2 and the Crystallographic Characterization of an Anilinium Chloride Thiocarbamate Adduct

Wafa Arar [1,2], Nuri Ekici [2], Michael Knorr [2,*], Isabelle Jourdain [2,*], Carsten Strohmann [3] and Jan-Lukas Kirchhoff [3]

1 Selective Organic-Heterocyclic Synthesis-Biological Activity Evaluation (LR17ESO01), Université de Tunis-El Manar, Tunis 2092, Tunisia; wafaarar22@gmail.com
2 Institut UTINAM UMR 6213 CNRS, Université de Franche-Comté, 16, Route de Gray, 25030 Besançon, France
3 Anorganische Chemie, Technische Universität Dortmund, Otto-Hahn Straße 6, 44227 Dortmund, Germany; carsten.strohmann@tu-dortmund.de (C.S.); jan-lukas.kirchhoff@tu-dortmund.de (J.-L.K.)
* Correspondence: michael.knorr@univ-fcomte.fr (M.K.); isabelle.jourdain@univ-fcomte.fr (I.J.); Tel.: +33-3-81-66-62-70 (M.K.)

Abstract: In order to investigate the coordination chemistry of *O*-alkyl *N*-aryl thiocarbamate ligands, HgI_2 was reacted with one equivalent of PrOC(=S)N(H)Ph **L** in toluene solution to afford the 1D polymeric title compound $[\{IHg(\mu\text{-}I)\}\{\kappa^1\text{-PrOC(=S)N(H)Ph}\}]_n$ **CP1**. The formation of this iodide-bridged coordination polymer was ascertained by a single-crystal X-ray diffraction study performed at 100 K, as well as the formation of an adduct between anilinium chloride and **L** forming a supramolecular ribbon of composition **[L(PhNH$_3$)(Cl)]**. The occurrence of anilinium chloride is due to the partial hydrolysis of **L** in the presence of HCl.

Keywords: mercury iodide; thiocarbamate; thione; crystal structure; anilinium salt

check for updates

Citation: Arar, W.; Ekici, N.; Knorr, M.; Jourdain, I.; Strohmann, C.; Kirchhoff, J.-L. Coordination of *O*-Propyl-*N*-phenylthiocarbamate to HgI_2 and the Crystallographic Characterization of an Anilinium Chloride Thiocarbamate Adduct. *Molbank* **2024**, *2024*, M1923. https://doi.org/10.3390/M1923

Academic Editor: Ian R. Baxendale

Received: 25 October 2024
Revised: 17 November 2024
Accepted: 19 November 2024
Published: 22 November 2024

1. Introduction

N-aryl-*O*-alkyl thiocarbamate ROC(=S)N(H)Ar constitute valuable intermediates in organic synthesis and these organosulfur compounds cover a wide range of applications, going from biological and pharmacological activity to catalysis [1–6]. Furthermore, they are also more and more used as ligands in coordination chemistry, since the soft C=S thione function (according Pearson's HSAB principle) [7] readily coordinates to numerous transition metals complexes with Cu(I), Ag(I), Hg(II), Ru(II), Rh(III), etc. [8–11]. Although most of these complexes are mononuclear, we have recently communicated the characterization of the dinuclear species $[\{I_2Bi(\mu_2\text{-}I)_2BiI_2\}\{\kappa^1\text{-MeOC(=S)N(H)Ph}\}_4]$ and that of the 1D-coordination polymers $[\{Cu(\mu_2\text{-}X)_2Cu\}\{\mu_2\text{-MeOC(=S)N(H)Ph}\}_2]_n$ (X Br, I) [12–14]. Some crystallographically characterized complexes ligated by *O*-alkyl-*N*-aryl thiocarbamates are presented in Scheme 1 [2,8,12].

Since some of our previously reported compounds ligated with MeOC(=S)N(H)Ph present only a limited solubility in common solvents, we decided to synthesize the already literature-known derivative PrOC(=S)N(H)Ph [15–17], which should assure, due its longer alkoxy chain, a better solubility. Furthermore, we are not aware of any metal complex bearing this thione-type ligand **L**. We therefore reacted HgI_2 with *O*-propyl-*N*-phenyl thiocarbamate and describe therein the crystal structure of the isolated coordination polymer. This research is a continuation of our investigations on the coordination chemistry of thioether and thione-type ligands on Hg(II) centers [18–21].

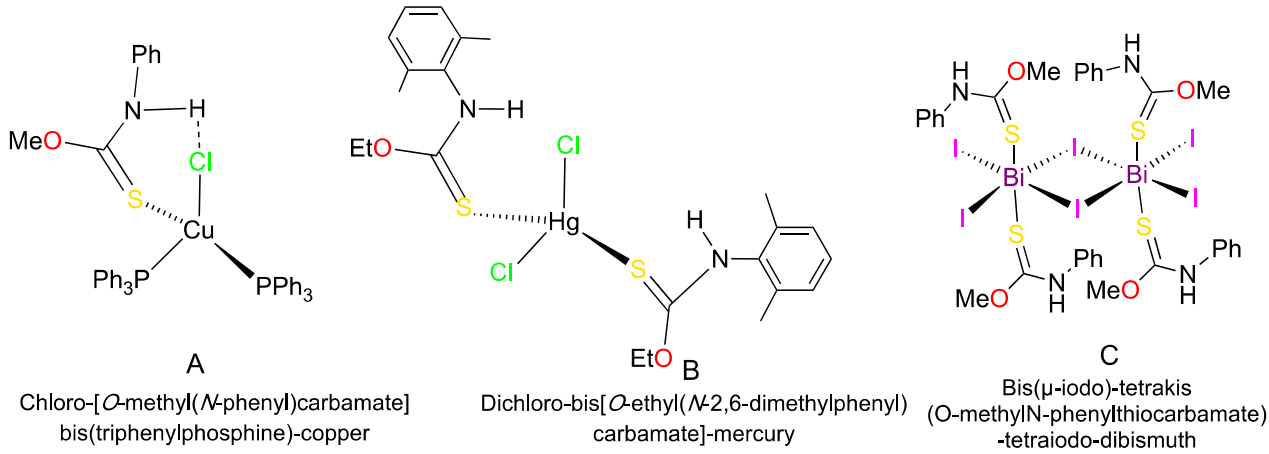

Scheme 1. Examples of some *O*-alkyl *N*-aryl thiocarbamate complexes.

2. Results and Discussion

The synthesis of PrOC(=S)N(H)Ph **L** has already been communicated by Tiekink et al., who obtained this thiocarbamate by the nucleophilic addition of in situ-generated sodium propanolate to phenylisothiocyanate, followed by acidic hydrolysis and extraction with $CHCl_3$ (Scheme 2) [16]. We applied the same protocol, but instead of performing the extraction 1 h after acidic hydrolysis with an excess of 2N HCl, we allowed the reaction mixture to stir overnight. According to the protocol in the literature, we then partially evaporated the chloroform extract, yielding a large amount of a yellowish, somewhat gluey solid. We picked up some yellowish crystals embedded in the crude product and noticed after a fast scan that the crystal parameters did not match with those reported by Tiekink et al. for crystalline **L**, which forms a dimer associated through strong N-H···S hydrogen bonds, giving rise to an eight-membered thioamide cycle. We therefore undertook a full crystal structure determination at 100 K, revealing a co-crystallization of **L** with anilinium chloride in a 1:1 ratio (Figure 1). The chloride anion of this anilinium salt, which probably originates partially from the hydrolysis of **L** after prolonged contact with aqueous HCl, interacts via hydrogen bonding with the three H atoms of the protonated aniline. The N2-H···Cl distances vary between 2.21 and 2.34 Å (d(N2···Cl^1) 3.2087(15) Å; d(N2···Cl) 3.1157(14) Å; d(N2···Cl^2) 3.1862(15) Å), and are somewhat looser than those reported for pure anilinum chloride (2.08–2.14 Å). Note that this latter salt is reported to form a layered supramolecular structure with $R_{63}(12)$ rings [22,23]. In the case of [**L**(PhNH$_3$)(Cl)], there is an additional bonding between the N1-H1 group of the thiocarbamate and the Cl^1 ion of 2.47 Å. Thus, a 1D supramolecular ribbon is generated. However, in contrast to the dimeric association reported for pure **L**, no secondary interactions between the thiocarbamate molecules are observed.

The ^{1}H NMR of pure recrystallized **L** recorded in $CDCl_3$ reveals at ambient temperature a broad signal at δ 4.56 for the OCH_2 group, whereas the CH_3 and CH_2 resonances are well resolved, appearing as a triplet and a sextet with a coupling constant of 7.2 Hz. Furthermore, the broad N-H resonance is found at δ 8.59 ppm. An indication of dynamic processes occurring in solution is provided by the ^{1}H NMR spectrum of **L** recorded at 323 K, in which the OCH_2 resonance at δ 4.56 appears now as a resolved triplet (Figure 2). There is also a slight low-field shift in the N-H signal. This dynamic behavior is probably due to a hindered rotation around the C-N bond, giving rise to conformational isomers. In the ^{13}C{^{1}H} NMR spectrum of **L**, the thiocarbonyl carbon is observed at δ 188.9 ppm, and the oxygen-bonded methylene group is observed at δ 74.8 (Figure 3).

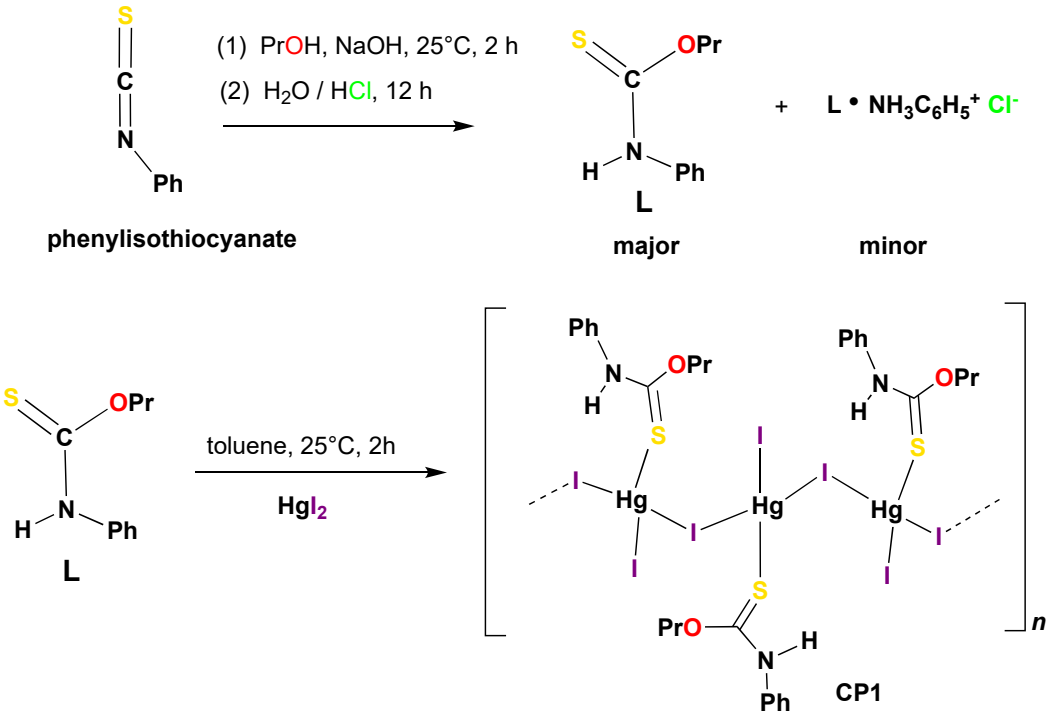

Scheme 2. Synthesis of **L** and **CP1**.

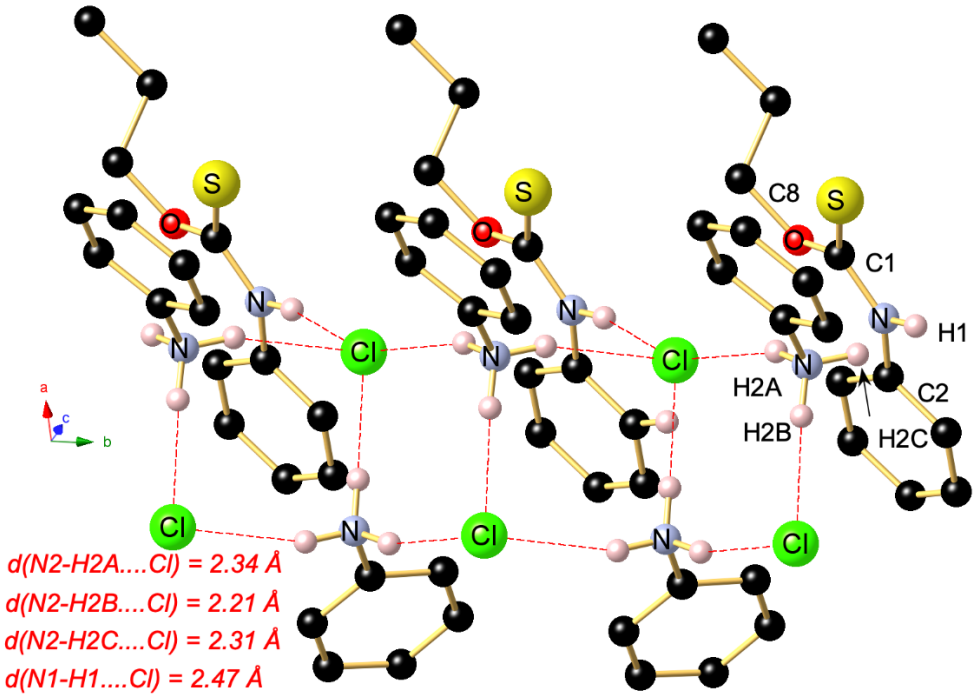

Figure 1. View of a segment of the supramolecular ribbon of PrOC(=S)NHPh•PhNH$_3$Cl running along the *b* axis. Selected bond lengths (Å) and angles (deg). S–C1 1.6697(16), O–C1 1.329(2), O–C8 1.457(2), N1–C1 1.348(2), N1–C2 1.418(2), N2–C11 1.4674(19), C6–C5 1.386(3); C1–O–C8 119.18(12), O–C8–C9 112.09(14), O–C1–S 125.73(12), O–C1–N1 112.85(14), N1–C1–S 121.41(13), C1–N1–C2 131.79(15), C3–C2–N1 125.38(15). N2–H2A···Cl^1 159.3, N2–H2B···Cl 171.5; N2–H2C···Cl^2 162.6, N1–H1···Cl^1 168.3. Symmetry transformation is used to generate equivalent atoms: ^{1}1/2-*x*, −1/2+*y*, 1/2-*z*; ^{2}1/2-*x*, 1/2 + *y*, 1/2-*z*.

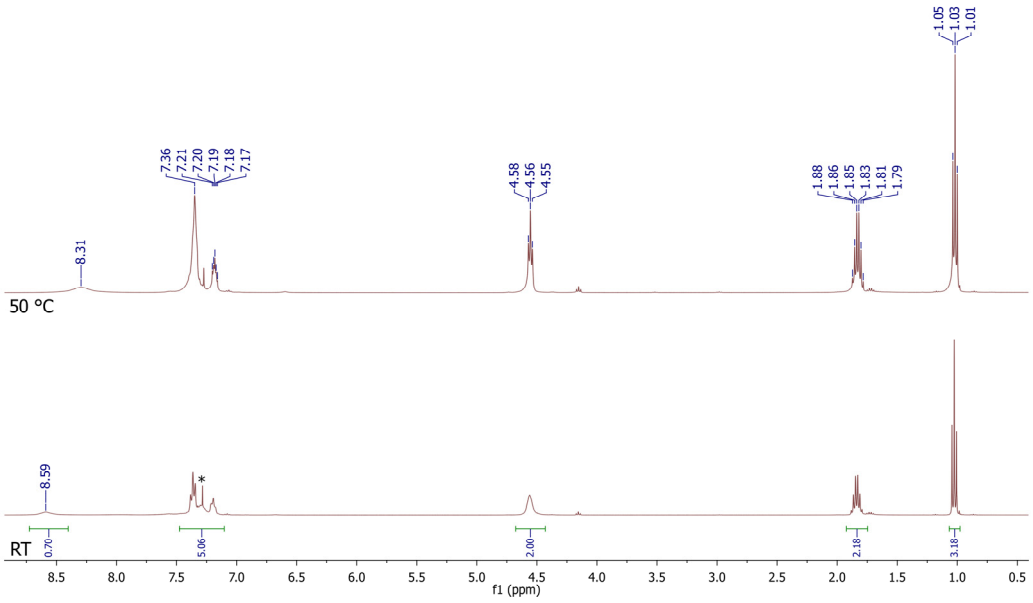

Figure 2. ^{1}H NMR spectra (400 MHz, $CDCl_3$) of **L** at 298 and 323 K. The * denotes $CHCl_3$.

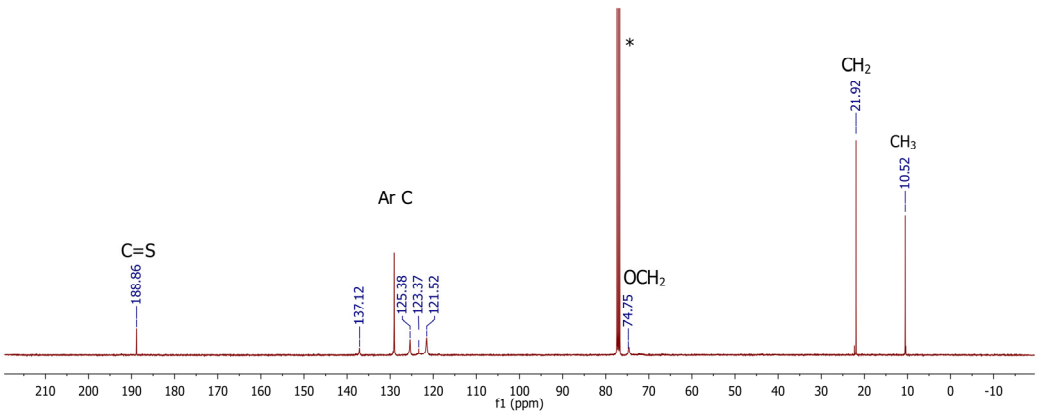

Figure 3. ^{13}C{^{1}H} NMR spectrum (100 MHz, $CDCl_3$) of **L** at 298 K. The * denotes $CDCl_3$.

The hitherto unknown polymeric HgI_2 complex [{IHg(μ-I)}{κ^1-PrOC(=S)N(H)Ph}] **CP1** shown in Scheme 2 was straightforwardly formed by adding at ambient temperature an equimolar amount of **L** to a slurry of HgI_2 in toluene. The orange-red suspension gradually dissolved after 2 h to give a homogenous solution. After layering with heptane, yellow-orange crystals were formed. This air-stable product is only partially soluble in $CDCl_3$, but the ^{1}H NMR spectrum clearly reveals a shift in the NH signal at δ 9.43 ppm to a lower field with respect to uncoordinated **L** (Δδ 0.84 ppm).

Since according to a survey in the literature only two tetrahedral molecular $HgCl_2$ complexes ligated by thiocarbamates have been crystallographically characterized yet [22,24], we examined the product crystallizing in the monoclinic space group $P2_1/c$ by an X-ray diffraction study performed at 100 K. As shown in Figure 4, a polymeric species has formed, in which the crystallographically identical coordinated Hg(II) centers are linked mutually through a μ_2-bridging I2 iodido ligand. The Hg···Hg separation of 4.22 Å excludes any intermetallic interaction.

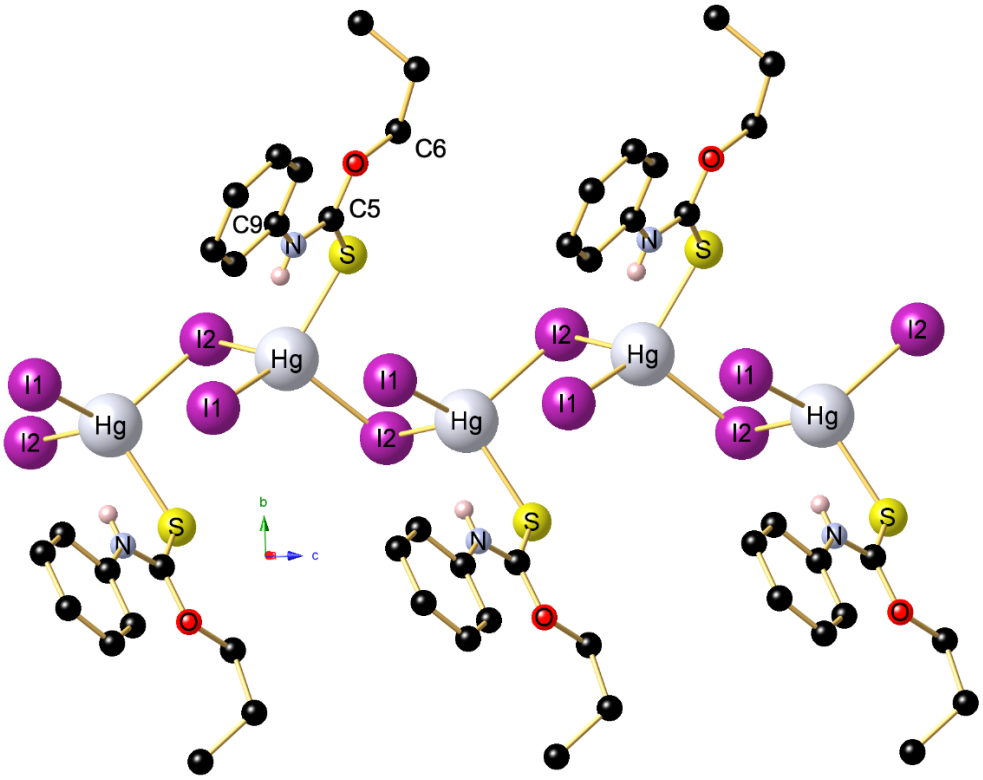

Figure 4. View of a segment of **CP1** running along the *c* axis. Selected bond lengths (Å) and angles (deg). Hg–I1 2.6829(3), Hg–I2 2.9073(3), Hg–I2^{1} 2.8421(3), Hg–S 2.5438(9), S–C5 1.710(4), O–C5 1.307(4), O–C6 1.473(4), N–C5 1.333(4), N–C9 1.430(4), C3–C7 1.390(5); I2^{1}–Hg1–I2 103.989(9), I1– Hg1–I2 106.923(9), I1–Hg1–2^{1} 116.402(9), S1–Hg1–I2^{1} 98.49(2), S1–Hg1–I2 102.18(2), S1–Hg1– I1 126.21(2), Hg1^{2-} I2-Hg 94.509(9), C5–O1–C6 120.0(3), C5–N1–C9 131.7(3), O–C5–S 121.5(3), O–C5–N 115.1(3), N–C5–S 123.4(3), O–C6–C10 105.9(3). Symmetry transformation is used to generate equivalent atoms: ^{1}+*x*, 1/2-*y*, 1/2 *z*; ^{2}+*x*, 1/2-*y*, −1/2+*z*.

The tetrahedral coordination sphere around each Hg atom is completed by a terminal I1 ligand and a S-bound thiocarbamate ligand. The Hg–S bond length of 2.5438(9) Å is significantly longer than the mean values of 2.44(1) and 2.499(1) Å reported for dichloro-bis(*O*-ethylthiocarbamato)mercury and dichloro-bis[*O*-ethyl(2,6-dimethylphenyl)thiocarbamato] mercury [22,24]. For comparison, for dinuclear bis[μ-iodo(thiobenzamide)mercury], a Hg–S bond length of 2.467(2) Å has been determined [25].

The C=S bond is slightly elongated with respect to that of non-ligated PrOC(=S)N(H)Ph (1.710(4), vs. 1.6697(16) Å). The bridging I2 atoms are quite symmetrically bridging, with the mean Hg–I_{bridg} bond distance of 2.875 Å being far longer than the Hg–I_{term} one (2.875 Å vs. 2.6829(3) Å). For the above-mentioned compound asymmetrical iodido-bridged [{IHg(μ_2-I)}{κ^1-thiobenzamide]$_2$, the respective Hg–I distances are 2.818(1), 3.201(1) and 2.673(1) Å [25]. At first glance, the 1D architectures of **CP1** and copper(I) analogue [{Cu(μ_2-I)$_2$Cu}(μ_2-EtOC(=S)N(H)Ph}**)**$_2$]$_n$ [15] are somewhat similar, but a closer look reveals some striking differences. The unidimensional ribbon of [{Cu(μ_2-I)$_2$Cu}{μ_2-EtOC(=S)N(H)Ph}$_2$] is doubly bridged by both μ_2-I atoms and bridging EtOC(=S)N(H)Ph ligands, bringing the metal centers into much closer contact. Furthermore, in the Cu(I) polymer chain, the N-H groups weakly interact with the μ_2-I atoms through an intramolecular N-H···I bonding of 2.778 Å, whereas in **CP1,** the shortest N-H···I contact is 3.143 Å

In the packing, no interchain interactions occur. Furthermore, as shown in Figure 5, loose intramolecular S···H and O···H contacts occur. Upon further examination of the molecular arrangement within the solid-state structure, it is noted that the polymer chain extends along a translational *c* glide symmetry. This is evident from the bonding of the HgI_2 salts with the respective thiocarbamate ligands. The positions of these ligands

alternate along the glide plane, while no significant intermolecular interactions, e.g., N1-H···Hg1, occur.

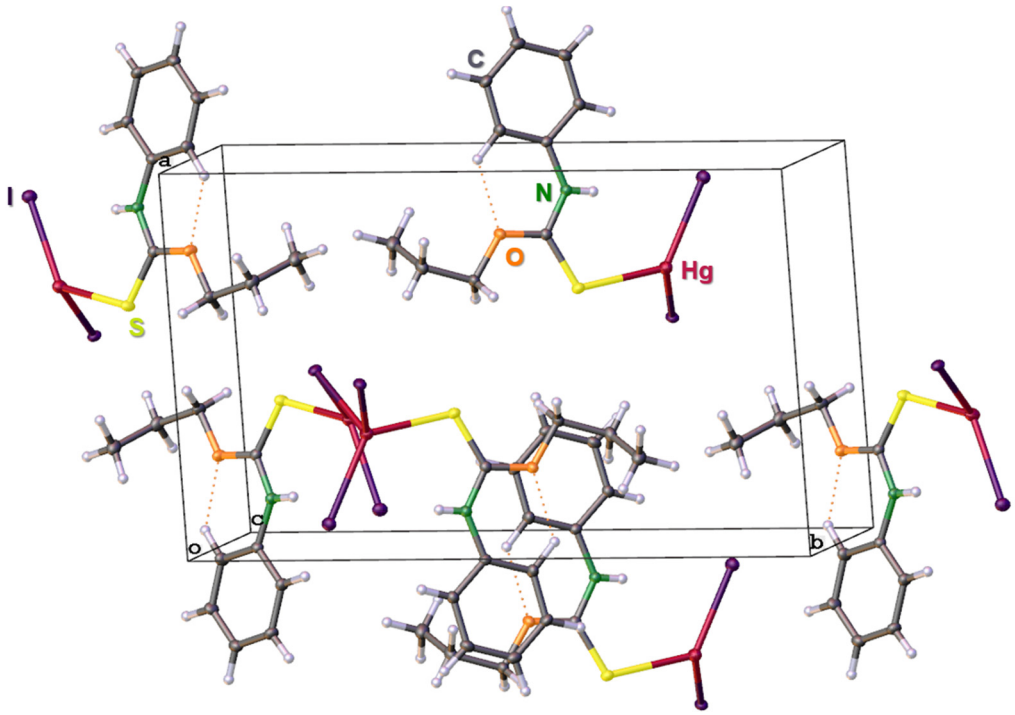

Figure 5. OLEX-generated view of the unit cell of **CP1**, indicating several intramolecular interactions by dotted lines (O2···H3C3 2.819(4) Å).

3. Experimental Methodology

*Synthesis of **CP1***—To a slurry of HgI_2 (454 mg, 1.0 mmol) in 10 mL of toluene, *O*-propyl *N*-phenylthiocarbamate **L** (195 mg, 1 mmol) was added in several portions. HgI_2 dissolved progressively and the reaction mixture was stirred at room temperature for 2 h. Then, the solvent was allowed to evaporate partially to about 6 mL. After layering with heptane, yellow-orange crystals of **CP1** were formed and then collected by filtration. Yield: 72%. Anal. Calc. for $C_{10}H_{13}HgI_2NOS$ (M.W. = 649.68 g·mol^{-1}): C, 18.49; H, 2.02; N, 2.16; S, 4.94%. Found: C, 18.32; H, 1.98; N, 2.11; S, 4.76%. IR-ATR: 1230 ν(C=S), 1483 ν(C–N), 1548 ν(N–H), 3281 ν(N–H bonded) cm^{-1}.

Data collection for **L** and **CP1** was performed on Bruker D8 Venture four-circle diffractometers from Bruker AXS GmbH (Karlsruhe, Germany). CPAD detectors used were Photon II (MoK$_\alpha$) and Photon III (AgK$_\alpha$) from Bruker AXS GmbH; X-ray sources: Microfocus source IμS; and microfocus source IμS Mo and Ag, respectively, from Incoatec GmbH with mirror optics HELIOS and a single hole collimator from Bruker AXS GmbH. Programs used for data collection were APEX4 Suite [26] (v2021.10-0) and integrated programs SAINT (V8.40A; integration) as well as SADABS (2018/7; absorption correction) from Bruker AXS GmbH [27]. The SHELX programs were used for further processing [28]. The solution of the crystal structures was achieved with the help of the program SHELXT [29], the structure refinement was achieved with SHELXL [30]. The processing and finalization of the crystal structure data was carried out with program OLEX2 v1.5 [31]. All non-hydrogen atoms were refined anisotropically. For the hydrogen atoms, the standard values of the SHELXL program were used with U_{iso} (H) = –1.2 U_{eq}(C) for CH_2 and CH and with U_{iso} (H) = –1.5 U_{eq}(C) for CH_3. All H atoms were refined freely using independent values for each U_{iso}(H).

Crystal data for $C_{16}H_{21}ClN_2OS$ **L** include the following: M = 324.86 g·mol^{-1}, colorless crystals, crystal size 0.343×0.287×0.156 mm^3, monoclinic, space group $P2_1/n$, a = 10.8275(14) Å, b = 5.6092(8) Å, c = 27.626(3) Å,), α = 90°, β = 94.473(5)°, γ = 90°, V = 1672.7(4)Å^3, Z = 4, D_{calc} = 1.290 g/cm^3, T = 100 K, λ = 0.71073, R_1 = 0.0343,

Rw_2 = 0.0838 for 43376 reflections with $I \geq 2\sigma(I)$ and 3412 independent reflections. Largest diff. peak/hole/e Å^{-3} 0.52/–0.22. A multi-scan absorption correction was applied; T_{max} = 0.4891, T_{min} = 0.3440.

Crystal data for $C_{10}H_{13}HgI_2NOS$ **CP1** include the following: M = 649.66 g·mol^{-1}, orange crystals, crystal size 0.216 × 0.169 × 0.117 mm^3, monoclinic, space group $P2_1/c$, a = 11.0287(7) Å, b = 17.3343(10) Å, c = 8.0027(5)Å), α = 90°, β = 101.7353(16)°, γ = 90°, V = 1497.93(16)Å^3, Z = 4, D_{calc} = 2.881 g/cm^3, T = 100 K, λ = 0.56086, R_1 = 0.0215, Rw_2 = 0.0473 for 73399 reflections with $I > = 2\sigma(I)$ and 4604 independent reflections. Largest diff. peak/hole/e Å^{-3} 1.55/–1.15. A multi-scan absorption correction was applied; T_{max} = 0.5624, T_{min} = 0.3964.

Data were collected using graphite-monochromated MoK_α radiation λ = 0.71073 Å and AgK_α radiation λ = 0.56086 Å. The structures were solved by intrinsic phasing and refined by full-matrix least-squares against F^2. Data have been deposited at the Cambridge Crystallographic Data Centre as CCDC 2382124 (**L**) and CCDC 2382127 (**CP1**) (Supplementary Materials). The data can be obtained free of charge from the Cambridge Crystallographic Data Centre via http://www.ccdc.cam.ac.uk/getstructures (accessed on 18 November 2024).

4. Conclusions

We have crystallographically evidenced that the reaction of PrOC(=S)N(H)Ph **L** with HgI_2 in a 1:1 ratio affords the 1D polymeric title compound $[\{IHg(\mu\text{-}I)\}\{\kappa^1\text{-}PrOC(=S)N(H)Ph\}]_n$ **CP1**. We are currently investigating whether changing the metal-to-ligand ratio may lead to a mononuclear tetrahedral species $[HgI_2\{PrOC(=S)N(H)Ph\}_2]$ that is similar to complex **A** shown in Scheme 1. We are also extending our investigation to other HgX_2 and CdX_2 salts.

Supplementary Materials: Crystallographic Data.

Author Contributions: W.A. and N.E. prepared the compound; C.S. and J.-L.K. collected the X-ray data and solved the structure; I.J. and M.K. designed the study, analyzed the data and wrote the paper. All authors have read and agreed to the published version of the manuscript.

Funding: This work has been achieved in the frame of the EIPHI Graduate school (contract "ANR-17-EURE-0002").

Data Availability Statement: The X-ray data are at CCDC as stated in the paper.

Acknowledgments: We thank Stéphanie Beffy for recording the IR and NMR spectra. C.S. and J.-L.K. thank the *Fonds der Chemischen Industrie* and the *Konrad-Adenauer-Stiftung* for financial support.

Conflicts of Interest: The authors declare no conflicts of interest.

References

1. Németh, A.G.; Keserű, G.M.; Ábrányi-Balogh, P. A novel three-component reaction between isocyanides, alcohols or thiols and elemental sulfur: A mild, catalyst-free approach towards *O*-thiocarbamates and dithiocarbamates. *Beilstein J. Org. Chem.* **2019**, *15*, 1523–1533. [CrossRef] [PubMed]
2. Zhang, J.; Zang, Q.; Yang, F.; Zhang, H.; Sun, J.Z.; Tang, B.Z. Sulfur Conversion to Multifunctional Poly(*O*-thiocarbamate)s through Multicomponent Polymerizations of Sulfur, Diols, and Diisocyanides. *J. Am. Chem. Soc.* **2021**, *143*, 3944–3950. [CrossRef]
3. Shadap, L.; Tyagi, J.L.; Poluri, K.M.; Novikov, S.; Timothy Lo, C.W.; Mozharivskyj, Y.; Kollipara, M.R. Insights to the strained thiocarbamate derivative complexes of platinum group metals induced by azide as a co-ligand: Characterization and biological studies. *J. Organomet. Chem.* **2020**, *920*, 121345. [CrossRef]
4. Krátký, M.; Volková, M.; Novotná, E.; Trejtnar, F.; Stolaříková, J.; Vinšová, J. Synthesis and biological activity of new salicylanilide N,N-disubstituted carbamates and thiocarbamates. *Bioorg. Med. Chem.* **2014**, *22*, 4073–4082. [CrossRef] [PubMed]
5. Tan, C.K.; Le, C.; Yeung, Y.Y. Enantioselective bromolactonization of *cis*-1,2-disubstituted olefinic acids using an amino-thiocarbamate catalyst. *Chem. Commun.* **2012**, *48*, 5793–5795. [CrossRef]
6. Šeršeň, F.; Král'ová, K.; Macho, V. New findings about the inhibitory action of phenylcarbamates and phenylthiocarbamates on photosynthetic apparatus. *Pestic. Biochem. Physiol.* **2000**, *68*, 113–118.
7. Pearson, R.G. Recent advances in the concept of hard and soft acids and bases. *J. Chem. Edu.* **1987**, *64*, 561–567. [CrossRef]
8. Yeo, C.I.; Halim, S.N.A.; Weng Ng, S.; Tan, S.L.; Zukerman-Schpector, J.; Ferreira, M.A.B.; Tiekink, E.R.T. Investigation of putative arene-C–H···π (quasi-chelate ring) interactions in copper(I) crystal structures. *Chem. Commun.* **2014**, *50*, 5984–5986. [CrossRef]

9. Yeo, C.I.; Teow, S.Y.; Liew, L.Y.; Chew, J.; Tiekink, E.R.T. Crystal structure of chlorido-(*O*-methyl phenylcarbamothioamide-κS)-bis(triphenylphosphane-κP)silver(I), $C_{44}H_{39}AgClNOP_2S$. *Z. Kristallogr. NCS* **2020**, *235*, 1473–1475. [CrossRef]
10. Nor, N.A.M.M.; Ahmad, J.; Abdullah, Z.; Halim, S.N.A.; Otero-de-la-Roza, A.; Tiekink, E.R.T. Bipodal benzoylthiocarbamic acid esters: Crystal and molecular structures of R = Et (a polymorph), and of a binuclear Cu(I) complex, R = iPr. *Z. Kristallogr.* **2014**, *230*, 397–405.
11. Furlani, C.; Tarantelli, T.; Gastaldi, L.; Porta, P. Complexing behaviour of thiocarbamic esters: Crystal and molecular structure of bis-(O-methyl phenylthiocarbamato)(triphenylphosphine)-palladium(II). *J. Chem. Soc. A* **1971**, 3778–3783. [CrossRef]
12. Arar, W.; Khatyr, A.; Knorr, M.; Strohmann, C.; Schmidt, A. Bis(μ-iodo)-tetrakis(*O*-methyl-*N*-phenylthiocarbamate)-tetraiodo-dibismuth. *Molbank* **2022**, *2022*, M1381. [CrossRef]
13. Arar, W.; Viau, L.; Jourdain, I.; Knorr, M.; Strohmann, C.; Scheel, R.; Ben Akacha, A. Synthesis of catena-bis(μ--bromo)-Synthesis of Catena-bis(μ-bromo)-(*O*-methyl-*N*-phenylthiocarbamate)-dicopper(I) and its reactivity towards PAr_3 (Ar = Ph, p-Tol). *Molbank* **2023**, *2023*, M1655. [CrossRef]
14. Arar, W.; Ben Ali, R.; Véronique El May, M.; Khatyr, A.; Jourdain, I.; Knorr, M.; Brieger, L.; Scheel, R.; Strohmann, C.; Chaker, A.; et al. Synthesis, crystal structures and biological activities of halogeno-(*O*-alkylphenylcarbamothioate) bis(triarylphosphine)copper (I) complexes. *J. Mol. Struct.* **2023**, *1284*, 135370. [CrossRef]
15. Besson, T.; Dozias, M.J.; Guillard, J.; Jacquault, P.; Legoy, M.D.; Rees, C.W. Expeditious Routes to 4-Alkoxyquinazoline-2-carbonitriles and Thiocarbamates via *N*-Ary l imino-l,2,3-dithiazoles Using Microwave Irradiation. *Tetrahedron* **1998**, *54*, 6475–6484. [CrossRef]
16. Sudkaow, P.; Yeo, C.I.; Weng, N.S.; Tiekink, E.R.T. O-Propyl N-phenylthiocarbamate. *Acta Cryst.* **2012**, *E68*, o1774. [CrossRef]
17. Sardarian, A.R.; Inaloo, I.D.; Zangiabadi, M. An Fe3O4@SiO2/Schiff base/Cu(II) complex as an efficient recyclable magnetic nanocatalyst for selective mono *N*-arylation of primary *O*-alkyl thiocarbamates and primary *O*-alkyl carbamates with aryl halides and arylboronic acids. *New J. Chem.* **2019**, *43*, 8557–8565. [CrossRef]
18. Arar, W.; Khatyr, A.; Knorr, M.; Brieger, L.; Krupp, A.; Strohmann, C.; Efrit, M.L.; Ben Akacha, A. Synthesis, Crystal Structures and Hirshfeld analyses of phosphonothioamidates $(EtO)_2P(=O)C(=S)N(H)R$ (R = Cy, Bz) and their coordination on CuI and HgX_2 (X = Br, I). *Phosphorus Sulfur Silicon Relat. Elem.* **2021**, *196*, 845–858. [CrossRef]
19. Hameau, A.; Guyon, F.; Knorr, M.; Enescu, M.; Strohmann, C. Self-Assembly of Dithiolene-based Coordination Polymers of Mercury(II): Dithioether versus Thiocarbonyl Bonding. *Monatsh. Chem.* **2006**, *137*, 545–555. [CrossRef]
20. Knorr, M.; Peindy, H.N.; Guyon, F.; Sachdev, H.; Strohmann, C. Synthesis and Molecular Structures of Platinum and Mercury Complexes Chelated by (Phenylthiomethyl)silane Ligands. *Z. Anorg. Allg. Chem.* **2004**, *630*, 1955–1961. [CrossRef]
21. Kinghat, R.; Khatyr, A.; Knorr, M.; Strohmann, C.; Kubicki, M.M. 4,4-Bis(isopropylthio)-1,1-diphenyl-2-azabuta-1,3-diene Adducts with Cadmium(II), Mercury(II) and Copper(I) Iodides: Crystal, Molecular and Electronic Structures of d^{10} Transition Metal Chelate Complexes. *Chemistry* **2024**, *6*, 62–80. [CrossRef]
22. Brown, C.J. The Crystal Structure of Aniline Hydrochloride. *Acta Gryst.* **1949**, *2*, 228. [CrossRef]
23. Lopez-Dupla, E.; Jones, P.G.; Vancea, F. Secondary Bonding Interactions in Some Di- and Trihaloanilinium Halides. *Z. Naturforsch.* **2003**, *58b*, 191–200. [CrossRef]
24. Bandoli, G.; Clemente, D.A.; Sindellari, L.; Tondello, E. Preparation, properties, and crystal structure of dichlorobis-(*O*-ethyl thiocarbamate)mercury(II). *J. Chem. Soc. Dalton Trans.* **1975**, 449–452. [CrossRef]
25. Hiller, W.; Castineiras, A.; Arquero, A.; Masaguer, J.R. Di-μ-iodo-bis[iodo(thiobenzamid-*S*)quecksilber(II)]. *Acta Cryst.* **1986**, *C42*, 151–153. [CrossRef]
26. Bruker. *Apex IV*; Bruker AXS Inc.: Madison, WI, USA, 2021.
27. Bruker. *SADABS*; Bruker AXS Inc.: Madison, WI, USA, 2001.
28. Sheldrick, G.M. A short history of SHELX. Acta Cryst. 2008, A64, 112−122. *Acta Cryst.* **2008**, *A64*, 112–122. [CrossRef]
29. Sheldrick, G.M. SHELXT—Integrated space-group and crystal-structure determination. *Acta Cryst.* **2015**, *A71*, 3–8. [CrossRef]
30. Sheldrick, G.M. Crystal structure refinement with SHELXL. *Acta Cryst.* **2015**, *C71*, 3–8.
31. Dolomanov, O.V.; Bourhis, L.J.; Gildea, R.J.; Howard, J.A.K.; Puschmann, H. OLEX2: A complete structure solution, refinement and analysis program. *J. Appl. Crystallogr.* **2009**, *42*, 339–341. [CrossRef]